

1 **Significance of perylene for source allocation of terrigenous organic** 2 **matter in aquatic sediments**

3
4
5 Ulrich M. Hanke^{1,*}, Ana L. Lima-Braun^{1,‡}, Timothy I. Eglinton^{1,2}, Jeffrey P. Donnelly³, Valier
6 Galy¹, Pascale Poussart^{1,†}, Konrad Hughen¹, Ann P. McNichol³, Li Xu³, Christopher M.
7 Reddy¹

8 ¹ Department of Marine Chemistry and Geochemistry, Woods Hole Oceanographic Institution,
9 266 Woods Hole Road, Woods Hole, MA 02543, USA

10 ² Geological Institute, ETH Zürich, Sonneggstrasse 5, 8092 Zurich, Switzerland

11 ³ Department of Geology and Geophysics, Woods Hole Oceanographic Institution, 266 Woods
12 Hole Road, Woods Hole, MA 02543, USA

13 [‡] Current address: ExxonMobil Exploration Company, Spring, Texas, USA

14 [†] Current address: Princeton University, 36 University Place, Princeton, New Jersey 08544
15 USA

16 *corresponding author: uhanke@whoi.edu
17
18
19
20
21
22

23 **ABSTRACT**

24
25 Perylene is a frequently abundant, and sometimes the only polycyclic aromatic hydrocarbon
26 (PAH) in aquatic sediments, but its origin has been subject of a longstanding debate in
27 geochemical research and pollutant forensics because its historical record differs markedly from
28 typical anthropogenic PAHs. Here we investigate whether perylene serves as a source-specific
29 molecular marker of fungal activity in forest soils. We use a well-characterized sedimentary

30 record (1735 to 1999) from the anoxic-bottom waters of the Pettaquamscutt River basin, RI,
31 USA to examine mass accumulation rates and isotope records of perylene, and compare them
32 with total organic carbon and the anthropogenic PAH fluoranthene. We support our arguments
33 with radiocarbon (^{14}C) data of higher plant leaf-wax *n*-alkanoic acids. Isotope-mass balance-
34 calculations of perylene and *n*-alkanoic acids indicate that ~40 % of sedimentary organic matter
35 is of terrestrial origin. Further, both terrestrial markers are pre-aged on millennial time-scales
36 prior to burial in sediments and insensitive to elevated ^{14}C concentrations following nuclear
37 weapons testing in the mid-20th Century. Instead, changes coincide with enhanced erosional
38 flux during urban sprawl. These findings suggest that perylene is definitely a product of soil-
39 derived fungi, and a powerful chemical tracer to study spatial and temporal connectivity
40 between terrestrial and aquatic environments.

41
42
43
44

INTRODUCTION

45 Perylene is found in marine ¹⁻⁵ and lacustrine sediments ⁶⁻⁸, in soils ^{9,10}, and also in petroleum
46 ^{11,12} and fuel emissions ^{13,14} often associated with other distinctive anthropogenic combustion-
47 derived polycyclic aromatic hydrocarbons (PAHs). However, most studies report that sediment
48 records of perylene differ greatly from those of anthropogenic PAHs ¹⁵⁻¹⁹. The latter are
49 typically most abundant in sediments post-dating the Industrial Revolution, particularly those
50 deposited during the latter half of the 20th Century, whereas perylene abundances are lowest
51 near the sediment-water interface and tend to increase with depth, particularly in anoxic
52 sedimentary settings ^{18,20}. This depth-related increase in concentration implies abiotic or
53 biologically mediated *in situ* production from precursor natural product(s) ^{2,21} by either a first-
54 or second-order reaction under anaerobic conditions ²⁰.

55
56
57
58
59
60
61
62
63
64
65
66
67
68
69
70
71
72
73
74
75
76
77
78

The origin of perylene has remained unclear for decades, during which has previously been argued for terrestrial^{1,2,22,23} and diagenetic^{6,16,24}, as well as petrogenic^{12,25} and pyrogenic^{13,14} sources. It was only recently that Itoh and collaborators²³ determined that the fungal species *Cenococcum geophyllum* produces 4,9-dihydroxyperylene-3,10-quinone, confirming a longstanding hypothesis^{1,22} that there is a naturally produced precursor. This ectomycorrhizal fungus appears almost ubiquitous in boreal, temperate and subtropical regions, and present in the rhizosphere of woody-plant roots and more generally in forest soils²⁶. A fungal origin can explain the widespread abundance of perylene in the environment even over geological time-scales²⁷, since mycorrhizal associations with vascular plants evolved about 400 million years ago²⁸.

Besides *C. geophyllum*, other mycorrhiza also produce similar perylene precursor compounds^{29,30} as toxins involved in pathogenesis of their host plant³¹. Prior stable carbon isotopic ($\delta^{13}\text{C}$) measurements of perylene found values similar to those terrestrial sources (C_3 -vegetation: $\delta^{13}\text{C} \approx -27\text{‰}$), supporting a wood-degrading origin from the rhizosphere³². This is further supported by dual-isotope analyses of perylene ($\delta^{13}\text{C}$ and δD) in sediments showing similar δD values as methoxy groups in lignin while $\delta^{13}\text{C}$ values are consistent with the expected fractionation range in saprophytic fungi²². In addition, natural abundance radiocarbon (^{14}C) analyses allows a comparison of the ^{14}C age of perylene with that of other organic matter constituents²⁵, including total organic carbon (TOC) and specific markers of terrigenous organic matter co-deposited in aquatic sediments. Such analyses shed light on the origin and provide further evidence on the origin of perylene and its use in environmental forensics.

79 Our motivation is to reconcile existing hypotheses on the source of perylene and assess the
80 potential of this marker compound as a biogeochemical tracer to follow the trajectories of
81 terrigenous organic matter mobilization and transport within watersheds. Specifically, we
82 investigate whether it serves as a molecular marker for rhizosphere carbon from catchment soils
83 and thus facilitates source approximation of terrigenous organic matter in sediments. Moreover,
84 while researchers currently tend to exclude perylene from forensic investigations involving the
85 apportionment of PAHs due to its incongruent behaviour, perylene may have mutagenic effects
86 on organisms^{33,34}. Thus, an improved understanding of the provenance and dynamics of
87 perylene may be pertinent to mapping inventories of natural and anthropogenic pollutants,
88 delineating transport pathways, and reconstructing historical land-use.

89
90 In this study, we construct historical records of perylene and TOC abundances and isotope
91 compositions from the anoxic sediments of the suburban Pettaquamscutt River basin, RI, USA.
92 We chose these sediments because they provide an exceptionally detailed chronological record
93 and a wealth of background information on the catchment area, including human influence on
94 local to regional scales^{15,35–38}. In addition, this sedimentary record extends over 260 years,
95 from the pre-industrial (~1735) until 1999, including an interval characterized by frequent
96 above-ground nuclear-bomb testing (resulting in elevated atmospheric ¹⁴C concentrations
97 peaking in 1963 when the testing ceased), thus offering the opportunity to study the rate at
98 which specific organic carbon species incorporate atmospheric CO₂ and are sequestered in
99 aquatic sediments. These characteristics of the study site, when coupled with down-core δ¹³C
100 and ¹⁴C records, provide a novel perspective on perylene biogeochemistry, yielding constraints
101 on its source and on the burial efficiency of terrigenous organic matter in aquatic sediments.
102 We compare mass accumulation rates (MAR) of perylene and TOC to the combustion-derived

103 PAH marker fluoranthene. While several non-alkylated PAHs could be used to trace past-
104 combustion practices, we choose fluoranthene because its quantitative down-core profile
105 resembles the temporal evolution of the sum of 15 parent PAHs in this watershed¹⁵. We further
106 support our interpretation with down-core data of particle size and leaf wax (C₃₀₋₃₂; *n*-alkanoic
107 acids) ¹⁴C variations. We then carefully assess whether the rhizosphere of wooded land serves
108 as the direct source for perylene in the environment and discuss the process of pre-ageing of
109 terrestrial organic matter prior to delivery into the aquatic environment in the context of parallel
110 sedimentary records.

111

112 **EXPERIMENTAL SECTION**

113 A series of seven freeze cores were collected in the depocenter of the lower basin of the
114 Pettaquamscutt River basin, RI, USA (41.503100; -71.450500) in 1999. The catchment area
115 covers 35 km² of forest, wetlands and open water of which today about 30 % is residential land
116 ³⁷. Ocean water flooded the basin about 1700 ± 300 years ago leading to a stratified water
117 column and sustained anoxic conditions in bottom waters and underlying sediments ³⁶. A
118 detailed description on the sediment chronology and sample processing is presented elsewhere
119 ^{15,39}. Sediment chronology was obtained from varve counting of x-ray radiographs as well as
120 from ¹³⁷Cs and ²¹⁰Pb profiles using the model of constant rate of supply that yielded a sequence
121 of about 260 years (1735-1999 AD) and an average sedimentation rate of 0.44 ± 0.10 cm yr⁻¹ ³⁹.

122

123 Sections from the cores were combined after aligning x-radiograph images including hurricane
124 layers in 1938 and 1954 to a reference chronology of varve counting, ²¹⁰Pb, and ¹³⁷Cs. This was
125 necessary to obtain enough sediment for trace molecular isotopic-analyses ³⁵. Hence, we pooled

126 the samples in eight horizons for all isotopic analyses: H1 (1999–1982), H2 (1981–1962), H3
127 (1960– 1931), H4 (1929–1898), and H5 (1896–1873), H6 (1871–1842), H7 (1840–1768), and
128 H8 (1764–1735) respectively, except *n*-alkanoic acids that were analyzed in four individual
129 samples: 1885±5, 1947±33, 1972±2, and 1991±1. Quantitative measurements for the
130 calculation of the mass accumulation rates as well as grain size analyses were performed on
131 individual samples as well.

132

133 **Grain size analyses**

134 One freeze-core slab was sub-sectioned using a scalpel blade, transferred into 50-mL round
135 bottom flasks and treated with a 30% hydrogen peroxide solution at a ratio of 40 ml per 1 g
136 sediment, and heated in a water bath to 70 °C as a means to support mineralization of the
137 organic matter. Subsequently, samples were freeze dried, and a subsample of about 11 mg was
138 suspended in water and measured on a Beckmann Coulter LS13 320 Laser Diffraction Particle
139 Analyser (Indianapolis, USA) in triplicate.

140

141 **Total Organic Carbon and Nitrogen**

142 A Fisons 1108 elemental analyzer was used to measure the TOC content of the samples. To
143 remove the inorganic carbon fraction, about 2 mg of dry sample was weighed into a silver
144 capsule and acidified with 20 µL of 2N HCl. TOC content was calculated in relation to the
145 whole sediment dry weight while organic carbon/organic nitrogen TOC/TN ratios were
146 calculated on an atomic basis. Samples were run in triplicate and all reported weight
147 percentages represent the mean ± one standard deviation with an instrumental blank of 0.004
148 mg for C and smaller than 0.005 mg for N.

149

150 **Isotope ratio monitoring mass spectrometry**

151 The stable carbon isotopic composition of bulk sample TOC was determined in triplicate by
152 automated on-line solid combustion interfaced to a Finnigan Delta Plus isotope ratio mass
153 spectrometer. Isotope ratios were calculated relative to CO₂ reference gas pulses, with standard
154 deviations for replicate measurements were always better than 0.6 ‰ and usually within 0.3 ‰.
155

156 **Extraction, purification and isotope analyses of perylene, fluoranthene and *n*-alkanoic
157 acids**

158 Dry sediment samples (0.5-1.5 g) were extracted by pressurized fluid extraction (Dionex ASE
159 200) using a mixture of acetone and *n*-hexane (1:1) at 1000 psi at 100 °C. Molecular
160 identification and quantification was achieved using an Agilent 6890 Plus GC System
161 interfaced to a mass selective detector operating at 70 eV in SIM mode using a DB-XLB
162 capillary column (60 m × 0.25 mm × 0.25 μm)¹⁵.

163
164 Compound-specific radiocarbon analyses (CSRA) of perylene and fluoranthene were performed
165 on eight pooled horizons by first using high-pressure liquid-chromatography (HPLC) to
166 separate pure perylene (98% purity or greater) from the sample extracts. The HPLC procedure
167 isolated PAHs into 2-ring and the combined 3+4-ring and 5+6-ring PAHs. The resulting 16
168 HPLC fractions (8 horizons x 2 ring classes) were subjected to two-dimensional preparative
169 capillary gas chromatography for isolation and purification of individual PAHs via HP 7683
170 auto-injector and a multi-column switching system (Gerstel MCS 2) connected to a HP 6890
171 series gas chromatograph, and Gerstel preparative fraction collector (PFC; further details in SI).
172 Purified samples were transferred to pre-combusted quartz tubes (7 mm I.D. x 20 cm), dried
173 under nitrogen before adding copper oxide (50 mg). Each tube was then evacuated on a vacuum

174 line while samples were kept at -90°C to prevent sublimation, sealed, and combusted at 850°C
175 for five hours. About 95% of the purified carbon dioxide was reduced to graphite, pressed and
176 analyzed for ^{14}C at NOSAMS, Woods Hole, U.S. and the remaining 5% was used for $\delta^{13}\text{C}$
177 measurements.

178

179 The $\delta^{13}\text{C}$ values of perylene were determined in triplicate on a Finnigan Delta Plus isotope ratio
180 mass spectrometer with attached Finnigan GC combustion III interface and Hewlett-Packard
181 6890 GC (irm-GC/MS). Compounds were separated on a CP-Sil 5CB capillary column (50 m \times
182 0.25 mm \times 0.25 μm) and isotope ratios for PAH peaks were calculated relative to CO_2
183 reference gas pulses. The standard deviation for replicate measurements of perylene was better
184 than 0.6 ‰ and mostly around 0.2 ‰.

185

186 The isotopic composition of leaf wax *n*-alkanoic acids (C_{30-32}) were determined for four
187 individual sediment samples deposited in 1885 \pm 5, 1947 \pm 33, 1972 \pm 2, and 1991 \pm 1 following the
188 analytical procedure described elsewhere ⁴⁰. In brief, *n*-alkanoic acids were extracted, isolated,
189 and purified using a preparative Hewlett Packard 5890 series II capillary gas chromatograph ⁴¹.
190 Following the chromatographic purification of individual compounds, samples were graphitized
191 and measured at NOSAMS, Woods Hole, U.S.

192

193 **Evaluation of isotope data**

194 Isotope mass-balance calculations provide quantitative estimates for source apportionment of
195 organic matter. To constrain the sources of TOC and perylene in Pettaquamscutt River
196 sediments, we calculated the relative contribution of possible organic carbon sources in the
197 sediments using the measured ^{14}C and $\delta^{13}\text{C}$ values for TOC (Figure 2). We report the ^{14}C data

198 as $F^{14}\text{C}$ which is the fraction modern independent from the year of measurement ⁴². We
199 assumed a simple mixing model to retrieve an average value for the lag-time of perylene and
200 leaf wax *n*-alkanoic acids; the details of which are published elsewhere ³⁵. In brief, these
201 source-specific molecular markers facilitate approximations of the contributions of terrigenous
202 organic matter in aquatic sediments (further details on the concept are included in SI).
203 To account for the potential variability under increasing human pressure on the coastal
204 environment, we determined average values of our terrestrial end-members for two time
205 periods: the pre-industrial (1735 to 1840) and the post-‘bomb’ (1960 to 1999) period (see SI for
206 more detail). Regarding ¹⁴C data evaluation, the post-1960s period also is a benchmark to test
207 for the resilience and short-term dynamics of catchment processes. In contrast, the aquatic end-
208 member is only affected by the marine reservoir effect, which is about 400 ± 40 ¹⁴C years lower
209 than the atmospheric ¹⁴C concentration at the time of burial ⁴³. Furthermore, we neglect a
210 potential impact of petrogenic carbon ⁴⁴ in the Pettaquamscutt River because of the absence of
211 post-glacial erosion and due to the absence of carbonaceous metasedimentary rocks in the basin
212 ⁴⁵. We constrain our model by $\delta^{13}\text{C} = -21.0$ ‰ for aquatic production ⁴⁶ and use local records of
213 perylene, pyrogenic carbon ³⁵ and *n*-alkanoic acids (C_{30-32}) to define terrestrial end-members.
214 We further obtained the contemporary atmospheric ¹⁴C concentrations from the extended
215 Intcal13 reference chronology ^{43,47}.

216

217 **RESULTS AND DISCUSSION**

218 The exceptionally well-constrained chronology of the Pettaquamscutt River sediments along
219 with detailed reconstructions of the provenance of combustion-derived PAHs ^{15,35} and Hg ³⁸
220 provide key constraints that allow us to determine whether perylene signatures are consistent
221 with its production in the rhizosphere of catchment soils ^{23,26}. To characterize the export of

222 terrigenous organic matter, including the putative precursors of perylene, and its subsequent
223 burial in aquatic sediments, we report MAR for TOC, perylene, and fluoranthene. Isotopic mass
224 balance calculations for $\delta^{13}\text{C}$ and ^{14}C records are employed to further constrain the main source
225 of perylene precursors. With reference to recent research and our results, we then provide a
226 synthesis aiming to merge the existing concepts, reconciling the origin of perylene (i.e.,
227 terrestrial, diagenetic or petro-/pyrogenic).

228

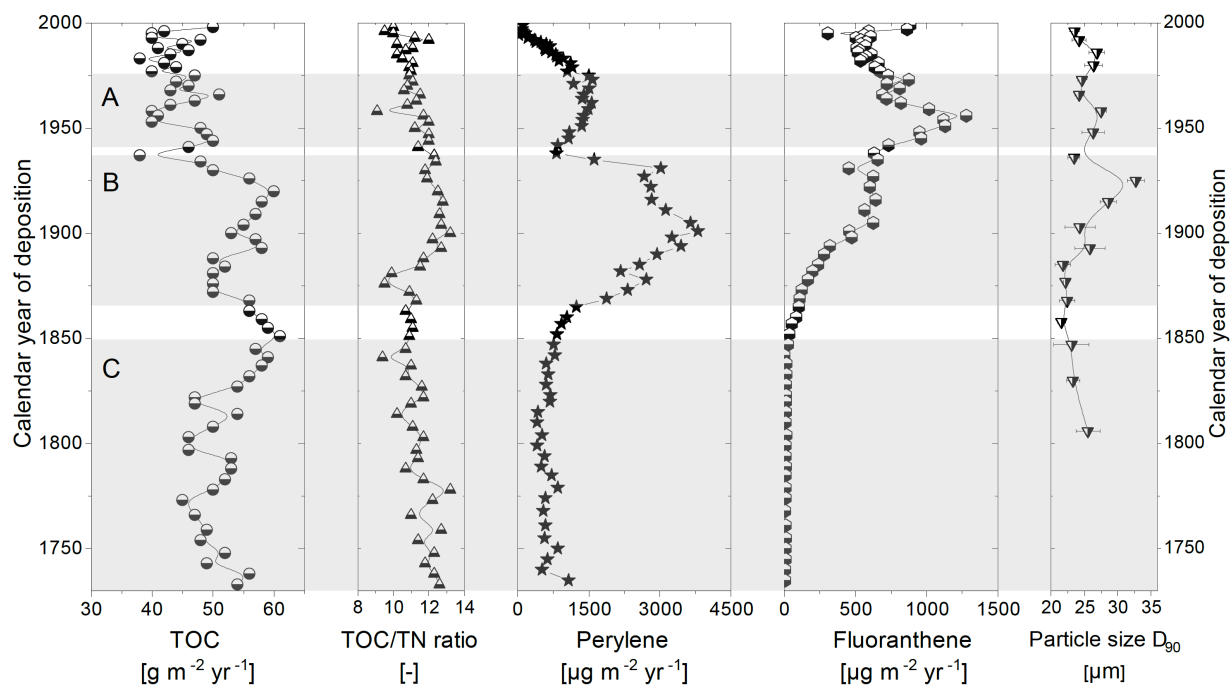
229 **Down-core mass accumulation rates of TOC and perylene**

230 The burial rate of TOC in the sediments of the Pettaquamscutt River ranges from 38 to 61 g m⁻²
231 yr⁻¹ (average = 49 ± 6 g m⁻² yr⁻¹, $n = 71$). The lowest TOC burial flux is observed in ca. 1938
232 (Figure 1) and is related to a 16.7 % shift in burial flux from 53.0 ± 43 g m⁻² yr⁻¹ prior to ca.
233 1927 to 44.0 ± 3.7 g m⁻² yr⁻¹ for sediments deposited thereafter. The timing of this change
234 coincides with the construction of the Lacey Bridge on the ocean side of the lower basin in
235 1934⁴⁵ (Figure 1B) that likely caused a restriction in seawater intrusion, affecting the influx of
236 both marine as well as the terrestrial matter. We argue that this exemplifies the accelerated
237 development of the catchment area beginning early in the last century and the related
238 infrastructure projects that changed the natural flow paths of materials within the watershed.

239

240 The N_{org} down-core record reveals only small variations, here illustrated as $C_{\text{org}}/N_{\text{org}}$ profiles (n
241 = 71; Figure 1) where three trends are delineated: decreasing C/N from 1730s (12.6) to 1840s
242 (9.4), a ~50-year reversal towards higher C/N ratios (13.2 in 1900), and a century-long C/N
243 secular decrease in the upper core (10.0 in 1999). This rather narrow range in C/N ratios
244 suggests that organic matter is predominantly yet not exclusively composed of labile material
245 with C/N values similar to aquatic organic matter (C/N = 4 to 10)⁴⁸. However, we refrain from

246 further speculations on this bulk-level information due to the absence of a robust reference for
 247 C/N values of terrigenous organic matter from this area.
 248



249
 250 Figure 1: Mass accumulation rates for total organic carbon (TOC), perylene, and fluoranthene as well as carbon to nitrogen
 251 (TOC/TN) ratios and down-core shifts in coarse particle abundance (D_{90}) with shaded area **A** representing the maximum PAH
 252 flux in this area, **B** the period of amplified erosion due to infrastructure development, and **C** the pre-industrial era prior to
 253 1840s.

254
 255 MARs for perylene/proto-perylene, which corresponds to the reduced perylene quinone, vary
 256 from 29 to $3800 \mu\text{g m}^{-2} \text{yr}^{-1}$, while its down-core profile differs markedly from the combustion-
 257 marker fluoranthene (Figure 1). The values were low before 1938, reached a maximum between
 258 ca. 1938 and 1973 ($1580 \mu\text{g m}^{-2} \text{yr}^{-1}$), before diminishing again in most recent decades (~ 100
 259 $\mu\text{g m}^{-2} \text{yr}^{-1}$) (Figure 1). This contrasting accumulation behaviour implies a different origin for
 260 perylene relative to combustion-derived PAHs, here illustrated by fluoranthene (Figure 1). This
 261 non-alkylated PAH appears lower in abundance varying from 1 to $1280 \mu\text{g m}^{-2} \text{yr}^{-1}$ and also

262 exhibits significant variability³⁵, however the temporal evolution of MARs of this pyrogenic
263 PAH differs sharply with that of perylene. Specifically, fluoranthene's MAR was low until the
264 mid-19th century (Figure 1C), increased steadily to a maximum in the late-1950s, then declined
265 in the post-1970s due to cleaner burning fuels and as consequence of environmental regulations
266^{15,37}. Such down-core profiles of combustion-derived PAHs are also observed in other
267 sedimentary records, including the upper basin of the Pettaquamscutt River^{16,19,49}.

268

269 The observed decline in perylene/proto-perylene MAR between 1927-1938 coincides with the
270 abrupt decrease in TOC accumulation rate (Figure 1B). We attribute the latter to a dilution in
271 organic carbon content resulting from a higher proportion of clastic material due to erosion of
272 soil mineral horizons (Figure 1). Perylene is a trace constituent of TOC, never accounting for
273 more than 0.1 % of TOC, and consequently perylene/TOC ratios shift by 500 % relative to
274 before or after this time interval. These observations thus support the link between a decrease in
275 perylene's MAR resulting from an increase in erosional flux (Figure 1B).

276

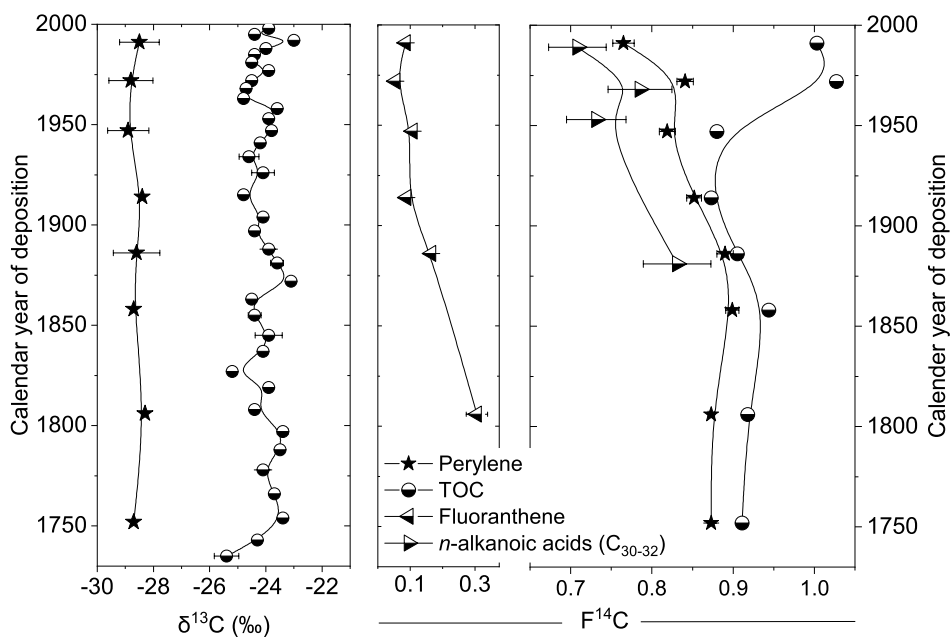
277 A striking feature of the perylene profile is that fluxes remain nearly constant ($665 \pm 180 \mu\text{g m}^{-2}$
278 yr^{-1} ; $n = 26$) prior to 1865, indicating either steady-state erosional conditions or quantitative
279 conversion of precursor material (Figure 1)²³. Due to the large variations in perylene burial
280 rates in our sedimentary record we refrain from attempting to derive kinetic parameters for
281 conversion of perylenequinone (proto-perylene) precursor to perylene. However, Slater and
282 collaborators⁵⁰ compared two perylene profiles from Lake Siskiwit collected in 1983 and 2005.
283 They found a reaction rate constant (0.048 yr^{-1}), ca. 75 % higher than previously reported²⁰
284 while another study reported much lower rates¹⁸. All of the above studies suggest that the
285 conversion of perylenequinone to perylene follows first-order kinetics. Nevertheless, the strong

286 (~ 97%) decrease in perylene abundance in Pettaquamscutt River sediments from 1973 to 1999
287 likely reflects incomplete conversion of precursor compounds (Figure 1).

288

289 **Isotope mass balance calculations**

290 The $\delta^{13}\text{C}$ TOC profile (Figure 2) appears relatively invariant throughout the core (-25.4 to -23.0
291 ‰, average -24.1 ± 0.5 ‰, $n = 36$), indicating the absence of large variations in organic matter
292 composition. Although the TOC MAR decreased in the 1930s, $\delta^{13}\text{C}$ values do not suggest this
293 was accompanied by a shift in the nature of organic matter supplied to Pettaquamscutt River
294 basin. Instead, the observed changes in burial flux in this catchment are attributed to a shift in
295 land use stemming from an increase in the local human population and the accompanied
296 development of infrastructure. The $\delta^{13}\text{C}$ values of perylene (-28.9 to -28.3 ‰; average $-28.6 \pm$
297 0.6 ‰; Figure 2) were similarly invariant, while significantly lower than TOC and similar to
298 that reported for terrestrial C_3 plants (-29 to -25, average -28 ‰) ⁵¹.



299 Figure 2: High-resolution $\delta^{13}\text{C}$ record for TOC and pooled sample results for perylene (left); molecular ^{14}C data for the
300 combustion-derived fluoranthene (middle) and results on perylene, leaf wax *n*-alkanoic acids as well as TOC (right).

301 In contrast, the ^{14}C record of TOC for pooled samples ($n = 8$; Figure 2) reveals only small
302 variations in pre-industrial time (1735 to 1840) but then tends to shift towards more ^{14}C
303 depleted values between 1839 and 1958. This change is thought to integrate the increasing use
304 of fossil fuels slightly diluting the natural atmospheric ^{14}C concentration (the so-called ‘Suess
305 effect’) as well as on-going infrastructural development and constructions within the catchment
306 resulting in the mobilization of deeper mineral soils. Thereafter, we observed a drastic (~15 %)
307 increase in $F^{14}\text{C}$ TOC values reflecting the shift in atmospheric ^{14}C derived from thermonuclear
308 weapons testing in the post-1960s. The uppermost sediment layer signals declining ^{14}C
309 concentrations similar to the atmosphere ⁴⁷.

310

311 Compound-specific radiocarbon analysis reveals that the ^{14}C profile of perylene follows that of
312 TOC from the pre-industrial period until ~1950. Thereafter, ^{14}C of TOC increases due to the
313 incorporation of atmospheric bomb ^{14}C , while perylene trends to more ^{14}C -depleted values.
314 This could reflect a pyrogenic (fossil fuel) contribution to perylene, mitigating the impact of
315 ‘bomb’ carbon in the Pettaquamscutt River sediments. However, CSRA of leaf wax *n*-alkanoic
316 acids (C_{30-32}) from the same sediments reveals a concomitant ^{14}C trend with perylene (Figure
317 2). We infer, therefore, that leaf waxes and perylene share a common source and mode of
318 export, implying that local erosional fluxes and mobilization of soil organic matter are
319 responsible for the decoupled TOC and perylene post-1950s signals rather than global-scale
320 perturbations such as ‘Suess effect’ or above-ground nuclear weapons testing.

321

322 In the mainly wooded catchment area of Pettaquamscutt River, organic molecules are produced
323 during photosynthetic activity, translocated and metabolized in plants, as well as released into
324 the rhizosphere. In the soil, plant and animal residues can be assimilated, stabilized and

325 metabolized until they eventually become respired to carbon dioxide ⁵², or they can be eroded
326 and redistributed within the watershed ⁵³. Source-specific molecular markers allow delineation
327 of specific processes associated with organic matter cycling, while molecular ¹⁴C data provide
328 additional information on the timescales of organic matter storage and transport from its source
329 to the ‘ultimate’ site of burial. This “residence time” has been determined for several markers
330 of terrestrial primary productivity ⁵⁴⁻⁵⁶, as well as charred plant biomass ^{35,57}, and range from
331 centuries to several millennia. The underlying processes resulting in organic matter ‘pre-aging’
332 prior to burial in aquatic depocenters can complicate source apportionment because the ¹⁴C
333 concentration of various organic matter components differs from that of the corresponding
334 atmospheric ¹⁴C reference value.

335

336 We determined an average ¹⁴C residence time for perylene of 1300 ± 300 ¹⁴C years for samples
337 pre-dating the industrialization (1735-1840, n = 3) and 2000 ± 500 ¹⁴C years for the post-
338 ‘bomb’ era (1960-1999; n = 3). These values agree well with leaf wax *n*-alkanoic acids (C₃₀₋₃₂)
339 that showed a 2700 ± 700 ¹⁴C year residence time for the post-‘bomb’ era (Figure 2), and a
340 record of biomass-derived pyrogenic carbon from the same core revealed an average age of
341 1460 ± 490 ¹⁴C years for the pre-industrial era ³⁵. The apparent average age or residence time
342 over the pre-industrial and the post-‘bomb’ era for perylene and higher plant *n*-alkanoic acids of
343 ca. 2000 ¹⁴C years is slightly higher than has been reported for (micro) charcoal in the same
344 catchment ³⁵ as well as for leaf wax *n*-alkanoic acids in the Bengal fan ⁵⁵ yet similar to that of
345 Cariaco basin ⁵⁶. However in the post-‘bomb’ era we observed a decoupling of ¹⁴C
346 concentrations among molecular markers and TOC. Specifically, the increase in atmospheric
347 ¹⁴C concentrations post-1960s is not apparent in perylene or *n*-alkanoic acids, suggesting that
348 soil carbon storage on millennial timescales may conceal or delay the legacy.

349

350 Isotope mass balance calculations based on TOC ^{13}C and ^{14}C data yield similar values for the
351 proportion of organic matter of terrestrial origin ($\delta^{13}\text{C}$: $-43 \pm 10 \%$ and ^{14}C : $-37 \pm 10 \%$), with
352 the remaining carbon derived from aquatic productivity. These results for the Pettaquamscutt
353 River basin are slightly higher than an estimated global average of one-third of sedimentary
354 organic of terrestrial origin⁵⁸. The similar estimates obtained from dual-carbon isotope
355 evaluations based on perylene reinforce its value in constraining the terrestrial end-member in
356 source apportionment.

357

358 **New constraints on the source of perylene**

359 The origin and widespread distribution of perylene in the environment has been a subject of
360 scientific debate for decades, although its conversion from the precursor molecule, 4,9-
361 dihydroxyperylene-3,10-quinone, has long been suspected^{1,2,23,29}. In particular, it has remained
362 unclear whether perylene is formed during *in-situ* diagenesis^{6,16} or is of petro-/pyrogenic origin
363^{11,14,25,59}. The former hypothesis was stimulated by the presence of perylene in Antarctic marine
364 sediments⁶⁰ and by large similarities between perylene and total organic matter down-core
365 profiles, fueling the notion of *in-situ* synthesis from TOC¹⁶. Along these lines, Gschwend and
366 collaborators²⁰ calculated kinetic parameters necessary to yield perylene from biogenic
367 precursor concentrations that are consistent with results from a recent study comparing down-
368 core profiles 20 years apart in Lake Siskiwit⁵⁰, and both are in line with the observed reduction
369 of perylenequinones²³. The second alternative hypothesis is based on the abundance of
370 perylene in ancient sediments^{22,61}, fossil fuels^{11,12} or combustion emissions^{13,14,59}. Regarding
371 the latter sources, perylene concentrations remain below 1.4% of the total PAH and thus are
372 negligible for the overall budget. Its presence in these matrices, however, raises the question of

373 whether perylene is exclusively of fungal origin. A possible explanation for the occurrence of
374 perylene in fossil fuels lies in the evolutionary development of fungi. The symbiotic interaction
375 between fungi and vascular plants evolved about 400 Ma ago, and ectomycorrhiza have existed
376 for at least 56 Ma ⁶², while the divergence and evolution of the mycorrhiza gene pool remains
377 largely unexplored ²⁸. However, Blumer proposed the conversion of pigments to hydrocarbons
378 through a geochemically irreversible deoxygenation of functional groups and hydrogenation
379 under sustained reducing conditions ⁶³. Even though this was exemplified for fossil crinoids in a
380 pigment-rich Triassic oil shale, these reactions likely also apply to the precursors of biogenic
381 PAH. We deduce, therefore, that fungal-derived perylenequinone is deoxygenated during
382 sediment diagenesis and, at least partly, survives coalification. This could explain the
383 occurrence of perylene in fossil deposits ³² and could explain its abundance in combustion
384 residues. One evolutionary rationale for the occurrence of perylene in sclerotia, the resting
385 structures of *C. geophyllum* ⁶⁴, is the extreme mutagenic activity of the unsaturated nucleus of
386 perylenequinones on gram-negative bacteria ³³, protecting the reproductive function of fungal
387 spores. Overall, the preponderance of evidence ^{17,22,32}, reinforced by our new data, indicates that
388 perylene is a remnant of wood degradation or fungal activity in the rhizosphere – a hotspot of
389 biological activity on land, and source of organic matter to aquatic systems.

390

391 **Parallels between perylene and TOC**

392 Sedimentary organic matter is a highly complex mixture composed of aquatic and terrigenous
393 organic carbon, and this complexity complicates source apportionment calculations, as well as
394 determination of carbon fluxes and thus the carbon burial efficiencies ^{65,66}. Measurement of the
395 abundance and isotopic composition of source-specific molecular markers can provide
396 constraints on terrigenous organic matter in sediments ⁶⁵. In addition to source constraints from

397 $\delta^{13}\text{C}$ and ^{14}C signatures, the latter also yields information on whether organic matter is of
398 modern or fossil origin⁴⁴, as well as on timescales of terrigenous organic matter between
399 formation on land and burial in aquatic depocenters (i.e., “average residence times”) ³⁵. The
400 process of ‘pre-aging’ implies a lag between biosynthesis and export of organic matter from
401 land to depocenter, with natural as well as anthropogenic molecules being retained in catchment
402 soils from annual to millennial time-scales ^{35,55,56}. Here, we find that this pre-aging process
403 occurs on similar time-scales for leaf wax fatty acids (*n*-alkanoic acids), biomass-derived
404 pyrogenic carbon and the rhizosphere tracer perylene – all together terrestrial markers with
405 different modes of formation, chemical structures and functionalities. This agreement between
406 these different source-specific markers suggests that retention within soils regulates the export
407 of most terrigenous organic matter and associated carbon-based pollutants that enter the soil
408 column.

409

410 TOC and perylene MARs co-vary in the pre-industrial era until about 1850 despite some
411 variability in the TOC flux (Figure 1). We attribute the latter to the increasing pressure by
412 extensive farming, as well as potential changes in aquatic productivity. The dual carbon isotope
413 records for TOC and perylene (Figure 2) support the absence of drastic compositional shifts
414 throughout the record, despite the influence of the ‘Suess effect’ and nuclear weapons testing
415 on the latter part of the TOC ^{14}C record. Notably, perylene shows large variation in MAR after
416 1850, which we suspect is due to the conversion of the catchment from a rural into a sub-urban
417 landscape that was accompanied by an enhanced erosional flux of carbon from bare soils.

418

419 Similarities between TOC and perylene records have been observed previously ^{6,16,22,61}, yet in
420 these cases it was suspected to reflect direct *in-situ* microbial production of perylene ¹⁶ rather

421 than the reduction and conversion of a precursor into perylene. This depletion of the precursor
422 pool may continue over geological time scales⁶³, thus limiting comprehensive quantitative
423 assessment of perylene in recent sediments⁵⁰. In contrast, the isotopic composition of perylene
424 is expected to be insensitive to conversion efficiency, and thus can serve as a robust tracer of
425 soil-derived terrestrial organic matter.

426

427 **Acknowledgement**

428 The authors thank John King, Sean Sylva, Brad Hubeny, Peter Sauer, Jim Broda for their help
429 in sampling, Carl Johnson and Daniel Montluçon for their incessant help with analyses as well
430 as Mark Yunker for critical discussion on the perils of perylene. Professor Phil Meyers and two
431 anonymous reviewers provided comments that improved the quality of the manuscript. U.M.H.
432 acknowledges the Swiss National Science Foundation for his postdoctoral fellowship and T.I.E.
433 and K.A.H. the NSF for research grants CHE-0089172 and OCE-9708478.

434

435 **Supporting Information.** Provides details on the preparative chromatographic isolation of
436 PAHs for compound-specific isotope analysis, the concept of two modes of terrigenous organic
437 matter export from land to oceans, the impact of the nuclear weapon testing on the atmospheric
438 and marine ¹⁴C partitioning over time and results for grain size analyses, respectively.

439

440 **Literature**

- 441 (1) Orr, W. L.; Grady, J. R. Perylene in Basin Sediments off Southern California. *Geochim.*
442 *Cosmochim. Acta* **1967**, *31*, 1201–1209. [https://doi.org/10.1016/S0016-7037\(67\)80058-](https://doi.org/10.1016/S0016-7037(67)80058-9)
443 9.
- 444 (2) Aizenshtat, Z. Perylene and Its Geochemical Significance. *Geochim. Cosmochim. Acta*

- 445 **1973**, *37*, 559–567. [https://doi.org/10.1016/0016-7037\(73\)90218-4](https://doi.org/10.1016/0016-7037(73)90218-4).
- 446 (3) Silliman, J. E.; Meyers, P. A.; Ostrom, P. H.; Ostrom, N. E.; Eadie, B. J. Insights into the
447 Origin of Perylene from Isotopic Analyses of Sediments from Saanich Inlet, British
448 Columbia. *Org. Geochem.* **2000**, *31* (11), 1133–1142. [https://doi.org/10.1016/S0146-](https://doi.org/10.1016/S0146-6380(00)00120-0)
449 6380(00)00120-0.
- 450 (4) Zhang, X.; Xu, Y.; Ruan, J.; Ding, S.; Huang, X. Origin, Distribution and Environmental
451 Significance of Perylene in Okinawa Trough since Last Glaciation Maximum. *Org.*
452 *Geochem.* **2014**, *76*, 288–294. <https://doi.org/10.1016/j.orggeochem.2014.09.008>.
- 453 (5) Venkatesan, M. I. Occurrence and Possible Sources of Perylene in Marine Sediments-a
454 Review *. *Mar. Chem.* **1988**, *25* (2845), 1–27. [https://doi.org/10.1016/0304-](https://doi.org/10.1016/0304-4203(88)90011-4)
455 4203(88)90011-4.
- 456 (6) Meyers, P. A.; Ishiwatari, R. Lacustrine Organic Geochemistry-an Overview of
457 Indicators of Organic Matter Sources and Diagenesis in Lake Sediments. *Org. Geochem.*
458 **1993**, *20* (7), 867–900. [https://doi.org/10.1016/0146-6380\(93\)90100-P](https://doi.org/10.1016/0146-6380(93)90100-P).
- 459 (7) Itoh, N.; Tamamura, S.; Kumagai, M. Distributions of Polycyclic Aromatic
460 Hydrocarbons in a Sediment Core from the North Basin of Lake Biwa, Japan. *Org.*
461 *Geochem.* **2010**, *41* (8), 845–852. <https://doi.org/10.1016/j.orggeochem.2010.04.002>.
- 462 (8) Gschwend, P. M.; Hites, R. A. Fluxes of Polycyclic Aromatic Hydrocarbons to Marine
463 and Lacustrine Sediments in the Northeastern United States. *Geochim. Cosmochim. Acta*
464 **1981**, *45* (12), 2359–2367. [https://doi.org/10.1016/0016-7037\(81\)90089-2](https://doi.org/10.1016/0016-7037(81)90089-2).
- 465 (9) Wilcke, W.; Krauss, M.; Amelung, W. Carbon Isotope Signature of Polycyclic Aromatic
466 Hydrocarbons (PAHs): Evidence for Different Sources in Tropical and Temperate
467 Environments? *Environ. Sci. Technol.* **2002**, *36* (16), 3530–3535.
468 <https://doi.org/10.1021/es020032h>.

- 469 (10) Gocht, T.; Barth, J. A. C.; Epp, M.; Jochmann, M.; Blessing, M.; Schmidt, T. C.;
470 Grathwohl, P. Indications for Pedogenic Formation of Perylene in a Terrestrial Soil
471 Profile: Depth Distribution and First Results from Stable Carbon Isotope Ratios. *Appl.*
472 *Geochemistry* **2007**, *22* (12), 2652–2663.
473 <https://doi.org/10.1016/j.apgeochem.2007.06.004>.
- 474 (11) Schnurmann, R.; Maddams, W. F.; Barlow, M. C. Spectrophotometric Identification of
475 Polynuclear Aromatic Components In High Boiling Petroleum Fractions. *Anal. Chem.*
476 **1953**, *25* (7), 1010–1013. <https://doi.org/10.1021/ac60079a003>.
- 477 (12) Wise, S. A.; Poster, D. L.; Leigh, S. D.; Rimmer, C. A.; Mössner, S.; Schubert, P.;
478 Sander, L. C.; Schantz, M. M. Polycyclic Aromatic Hydrocarbons (PAHs) in a Coal Tar
479 Standard Reference Material-SRM 1597a Updated. *Anal. Bioanal. Chem.* **2010**, *398* (2),
480 717–728. <https://doi.org/10.1007/s00216-010-4008-x>.
- 481 (13) Simoneit, B. R. T.; Rogge, W. F.; Lang, Q.; Jaffé, R. Molecular Characterization of
482 Smoke from Campfire Burning of Pine Wood (*Pinus Elliottii*). *Chemosph. - Glob.*
483 *Chang. Sci.* **2000**, *2* (1), 107–122. [https://doi.org/10.1016/S1465-9972\(99\)00048-3](https://doi.org/10.1016/S1465-9972(99)00048-3).
- 484 (14) Wang, Z.; Fingas, M.; Shu, Y. Y.; Sigouin, L.; Landriault, M.; Lambert, P.; Turpin, R.;
485 Campagna, P.; Mullin, J. Quantitative Characterization of PAHs in Burn Residue and
486 Soot Samples and Differentiation of Pyrogenic PAH1 from Petrogenic PAHs - The 1994
487 Mobile Burn Study. *Environ. Sci. Technol.* **1999**, *33* (18), 3100–3109.
488 <https://doi.org/10.1021/es990031y>.
- 489 (15) Lima, A. L.; Eglinton, T. I.; Reddy, C. M. High-Resolution Record of Pyrogenic
490 Polycyclic Aromatic Hydrocarbon Deposition during the 20th Century. *Environ. Sci.*
491 *Technol.* **2003**, *37* (1), 53–61. <https://doi.org/10.1021/es025895p>.
- 492 (16) Silliman, J. E.; Meyers, P. A.; Eadie, B. J.; Val Klump, J. A Hypothesis for the Origin of

- 493 Perylene Based on Its Low Abundance in Sediments of Green Bay, Wisconsin. *Chem.*
494 *Geol.* **2001**, *177* (3–4), 309–322. [https://doi.org/10.1016/S0009-2541\(00\)00415-0](https://doi.org/10.1016/S0009-2541(00)00415-0).
- 495 (17) Wakeham, S. G.; Canuel, E. A. Biogenic Polycyclic Aromatic Hydrocarbons in
496 Sediments of the San Joaquin River in California (USA), and Current Paradigms on
497 Their Formation. *Environ. Sci. Pollut. Res.* **2016**, *23* (11), 10426–10442.
498 <https://doi.org/10.1007/s11356-015-5402-x>.
- 499 (18) Fan, C. W.; Shiue, J.; Wu, C. Y.; Wu, C. Y. Perylene Dominance in Sediments from a
500 Subtropical High Mountain Lake. *Org. Geochem.* **2011**, *42* (1), 116–119.
501 <https://doi.org/10.1016/j.orggeochem.2010.10.008>.
- 502 (19) Hites, R. A.; Laflamme, R. E.; Windsor, J. G.; Farrington, J. W.; Deuser, W. G.
503 Polycyclic Aromatic Hydrocarbons in an Anoxic Sediment Core from the
504 Pettaquamscutt River (Rhode Island, U.S.A.). *Geochim. Cosmochim. Acta* **1980**, *44* (6),
505 873–878. [https://doi.org/10.1016/0016-7037\(80\)90267-7](https://doi.org/10.1016/0016-7037(80)90267-7).
- 506 (20) Gschwend, P. M.; Chen, P. H.; Hites, R. A. On the Formation of Perylene in Recent
507 Sediments: Kinetic Models. *Geochim. Cosmochim. Acta* **1983**, *47* (12), 2115–2119.
508 [https://doi.org/10.1016/0016-7037\(83\)90036-4](https://doi.org/10.1016/0016-7037(83)90036-4).
- 509 (21) Wakeham, S. G. Synchronous Fluorescence Spectroscopy and Its Application to
510 Indigenous and Petroleum-Derived Hydrocarbons in Lacustrine Sediments. *Environ. Sci.*
511 *Technol.* **1977**, *11* (3), 272–276. <https://doi.org/10.1021/es60126a012>.
- 512 (22) Grice, K.; Lu, H.; Atahan, P.; Asif, M.; Hallmann, C.; Greenwood, P.; Maslen, E.;
513 Tulipani, S.; Williford, K.; Dodson, J. New Insights into the Origin of Perylene in
514 Geological Samples. *Geochim. Cosmochim. Acta* **2009**, *73* (21), 6531–6543.
515 <https://doi.org/10.1016/j.gca.2009.07.029>.
- 516 (23) Itoh, N.; Sakagami, N.; Torimura, M.; Watanabe, M. Perylene in Lake Biwa Sediments

- 517 Originating from Cenococcum Geophilum in Its Catchment Area. *Geochim. Cosmochim.*
518 *Acta* **2012**, *95*, 241–251. <https://doi.org/10.1016/j.gca.2012.07.037>.
- 519 (24) Louda, J. W.; Baker, E. W. Perylene Occurrence, Alkylation and Possible Sources in
520 Deep-Ocean Sediments. *Geochim. Cosmochim. Acta* **1984**, *48* (5), 1043–1058.
521 [https://doi.org/10.1016/0016-7037\(84\)90195-9](https://doi.org/10.1016/0016-7037(84)90195-9).
- 522 (25) Jautzy, J. J.; Ahad, J. M. E.; Hall, R. I.; Wiklund, J. A.; Wolfe, B. B.; Gobeil, C.; Savard,
523 M. M. Source Apportionment of Background PAHs in the Peace-Athabasca Delta
524 (Alberta, Canada) Using Molecular Level Radiocarbon Analysis. *Environ. Sci. Technol.*
525 **2015**, *49* (15), 9056–9063. <https://doi.org/10.1021/acs.est.5b01490>.
- 526 (26) Obase, K.; Douhan, G. W.; Matsuda, Y.; Smith, M. E. Progress and Challenges in
527 Understanding the Biology, Diversity, and Biogeography of Cenococcum Geophilum. In
528 *Biogeography of Mycorrhizal Symbiosis*; Tedersoo, L., Ed.; Springer International
529 Publishing, 2017; Vol. Ecological, pp 299–318. [https://doi.org/10.1007/978-3-319-](https://doi.org/10.1007/978-3-319-56363-3)
530 [56363-3](https://doi.org/10.1007/978-3-319-56363-3).
- 531 (27) Suzuki, N.; Yessalina, S.; Kikuchi, T. Probable Fungal Origin of Perylene in Late
532 Cretaceous to Paleogene Terrestrial Sedimentary Rocks of Northeastern Japan as
533 Indicated from Stable Carbon Isotopes. *Org. Geochem.* **2010**, *41* (3), 234–241.
534 <https://doi.org/10.1016/j.orggeochem.2009.11.010>.
- 535 (28) Strullu-Derrien, C.; Selosse, M. A.; Kenrick, P.; Martin, F. M. The Origin and Evolution
536 of Mycorrhizal Symbioses: From Palaeomycology to Phylogenomics. *New Phytol.* **2018**,
537 *220* (4), 1012–1030. <https://doi.org/10.1111/nph.15076>.
- 538 (29) Allport, D. C.; Bu'Lock, J. D. Biosynthetic Pathways in *Daldinia Concentrica*. *J. Chem.*
539 *Soc.* **1960**, No. 654–662. <https://doi.org/10.1039/JR9600000654>.
- 540 (30) Wu, H.; Lao, X. F.; Wang, Q. W.; Ren-Rong, L.; Shen, C.; Zhang, F.; Liu, M.; Jia, L.

- 541 The Shiraiachromes: Novel Fungal Perylenequinone Pigments from *Shiraia*
542 *Bambusicola*. *J. Nat. Prod.* **1989**, *52* (5), 948–951. <https://doi.org/10.1021/np50065a006>.
- 543 (31) Daub, M. E.; Herrero, S.; Chung, K. R. Photoactivated Perylenequinone Toxins in
544 Fungal Pathogenesis of Plants. *FEMS Microbiol. Lett.* **2005**, *252* (2), 197–206.
545 <https://doi.org/10.1016/j.femsle.2005.08.033>.
- 546 (32) Marynowski, L.; Smolarek, J.; Bechtel, A.; Philippe, M.; Kurkiewicz, S.; Simoneit, B. R.
547 T. Perylene as an Indicator of Conifer Fossil Wood Degradation by Wood-Degrading
548 Fungi. *Org. Geochem.* **2013**, *59*, 143–151.
549 <https://doi.org/10.1016/j.orggeochem.2013.04.006>.
- 550 (33) Kaden, D. A.; Hites, R. A.; Thilly, W. G. Mutagenicity of Soot and Associated
551 Polycyclic Aromatic Hydrocarbons to *Salmonella Typhimurium*. *Cancer Res.* **1979**, *39*
552 (10), 4152–4159. <https://doi.org/10.1109/ICDM.2018.00085>.
- 553 (34) United States Environmental Protection Agency. *Provisional Peer Reviewed Toxicity*
554 *Values for Perylene (CASRN 198-55-0)*; Cincinnati, 2006.
- 555 (35) Hanke, U. M.; Reddy, C. M.; Braun, A. L. L.; Coppola, A. I.; Haghypour, N.; McIntyre,
556 C. P.; Wacker, L.; Xu, L.; McNichol, A. P.; Abiven, S.; Schmidt, M. W. I.; Eglinton, T.
557 I. What on Earth Have We Been Burning? Deciphering Sedimentary Records of
558 Pyrogenic Carbon. *Environ. Sci. Technol.* **2017**, *51* (21), 12972–12980.
559 <https://doi.org/10.1021/acs.est.7b03243>.
- 560 (36) Hubeny, J. B.; King, J. W.; Cantwell, M. Anthropogenic Influences on Estuarine
561 Sedimentation and Ecology: Examples from the Varved Sediments of the Pettaquamscutt
562 River Estuary, Rhode Island. *J. Paleolimnol.* **2009**, *41*, 297–314.
563 <https://doi.org/10.1007/s10933-008-9226-2>.
- 564 (37) Hanke, U. M.; Eglinton, T. I.; Braun, A. L. L.; Reddy, C. M.; Wiedemeier, D. B.;

- 565 Schmidt, M. W. I. Decoupled Sedimentary Records of Combustion: Causes and
566 Implications. *Geophys. Res. Lett.* **2016**, *43* (10), 5098–5108.
567 <https://doi.org/10.1002/2016GL069253>.
- 568 (38) Fitzgerald, W. F.; Engstrom, D. R.; Hammerschmidt, C. R.; Lamborg, C. H.; Balcom, P.
569 H.; Lima-Braun, A. L.; Bothner, M. H.; Reddy, C. M. Global and Local Sources of
570 Mercury Deposition in Coastal New England Reconstructed from a Multiproxy, High-
571 Resolution, Estuarine Sediment Record. *Environ. Sci. Technol.* **2018**, *52* (14), 7614–
572 7620. <https://doi.org/10.1021/acs.est.7b06122>.
- 573 (39) Lima, A. L.; Hubeny, J. B.; Reddy, C. M.; King, J. W.; Huguen, K. A.; Eglinton, T. I.
574 High-Resolution Historical Records from Pettaquamscutt River Basin Sediments: 1.
575 ²¹⁰Pb and Varve Chronologies Validate Record of ¹³⁷Cs Released by the Chernobyl
576 Accident. *Geochim. Cosmochim. Acta* **2005**, *69* (7), 1803–1812.
577 <https://doi.org/10.1016/j.gca.2004.10.009>.
- 578 (40) Drenzek, N. J.; Montluçon, D. B.; Yunker, M. B.; Macdonald, R. W.; Eglinton, T. I.
579 Constraints on the Origin of Sedimentary Organic Carbon in the Beaufort Sea from
580 Coupled Molecular ¹³C And ¹⁴C Measurements. *Mar. Chem.* **2007**, *103* (1–2), 146–162.
581 <https://doi.org/10.1016/j.marchem.2006.06.017>.
- 582 (41) Eglinton, T. I.; Aluwihare, L. I.; Bauer, J. E.; Druffel, E. R. M.; McNichol, A. P. Gas
583 Chromatographic Isolation of Individual Compounds from Complex Matrices for
584 Radiocarbon Dating. *Anal. Chem.* **1996**, *68*, 904–912.
585 <https://doi.org/10.1021/ac9508513>.
- 586 (42) Reimer, P. J.; Brown, T. A.; Reimer, R. W. Discussion: Reporting and Calibration of
587 Post-Bomb ¹⁴C Data. *Radiocarbon* **2004**, *46* (3), 1299–1304.
588 https://doi.org/10.2458/azu_js_rc.46.4183.

- 589 (43) Reimer, P. J.; Bard, E.; Bayliss, A.; Beck, J. W.; Blackswell, P. G.; Ramsey, C. B.; Buck,
590 C. E.; Cheng, H.; Edwards, R. L.; Friedrich, M.; Grootes, P. M.; Guilderson, T. P.;
591 Haflidason, H.; Hajdas, I.; Hatté, C.; Heaton, T. J.; Hoffmann, D. L.; Hogg, A. G.;
592 Hughen, K. A.; Kaiser, K. F.; Kromer, B.; Manning, S. W.; Niu, M.; Reimer, R. W.;
593 Richards, D. A.; Scott, E. M.; Southon, J. R.; Staff, R. A.; Turney, C. S. M.; van der
594 Pflicht, J. Intcal13 and Marine13 Radiocarbon Age Calibration Curves 0-50,000 Years
595 Cal BP. *Radiocarbon* **2013**, *55* (4), 1869–1887.
596 https://doi.org/10.2458/azu_js_rc.55.16947.
- 597 (44) Blattmann, T. M.; Letsch, D.; Eglinton, T. I. On the Geological and Scientific Legacy of
598 Petrogenic Organic Carbon. *Am. J. Sci.* **2018**, *318* (8), 861–881.
599 <https://doi.org/10.2475/08.2018.02>.
- 600 (45) Gaines, A. G. Papers on the Geomorphology, Hydrography and Geochemistry of the
601 Pettaquamscutt River Estuary. PhD Dissertation, University of Rhode Island, 1975.
- 602 (46) Meyers, P. A. Preservation of Elemental and Isotopic Source Identification of
603 Sedimentary Organic Matter. *Chem. Geol.* **1994**, *114* (3–4), 289–302.
604 [https://doi.org/10.1016/0009-2541\(94\)90059-0](https://doi.org/10.1016/0009-2541(94)90059-0).
- 605 (47) Levin, I.; Kromer, B.; Hammer, S. Atmospheric D14CO2 Trend in Western European
606 Background Air from 2000 to 2012. *Tellus B* **2013**, *65* (20092), 1–7.
607 <https://doi.org/10.3402/tellusb.v65i0.20092>.
- 608 (48) Meyers, P. A. Organic Geochemical Proxies of Paleoceanographic, Paleolimnologic, and
609 Paleoclimatic Processes. *Org. Geochem.* **1997**, *27* (5/6), 213–250.
610 [https://doi.org/10.1016/S0146-6380\(97\)00049-1](https://doi.org/10.1016/S0146-6380(97)00049-1).
- 611 (49) Tan, Y. L.; Heit, M. Biogenic and Abiogenic Polynuclear Aromatic Hydrocarbons in
612 Sediments from Two Remote Adirondack Lakes. *Geochim. Cosmochim. Acta* **1981**, *45*

- 613 (11), 2267–2279. [https://doi.org/10.1016/0016-7037\(81\)90076-4](https://doi.org/10.1016/0016-7037(81)90076-4).
- 614 (50) Slater, G. F.; Benson, A. A.; Marvin, C.; Muir, D. PAH Fluxes to Siskiwit Revisited:
615 Trends in Fluxes and Sources of Pyrogenic PAH and Perylene Constrained via
616 Radiocarbon Analysis. *Environ. Sci. Technol.* **2013**, *47* (10), 5066–5073.
617 <https://doi.org/10.1021/es400272z>.
- 618 (51) O’Leary, M. Carbon Isotopes in Photosynthesis. *Bioscience* **1988**, *38* (5), 328–336.
619 <https://doi.org/10.2307/1310735>.
- 620 (52) Lehmann, J.; Kleber, M. The Contentious Nature of Soil Organic Matter. *Nature* **2015**,
621 *528*, 60–68. <https://doi.org/10.1038/nature16069>.
- 622 (53) Berhe, A. A.; Barnes, R. T.; Six, J.; Marín-Spiotta, E. Role of Soil Erosion in
623 Biogeochemical Cycling of Essential Elements: Carbon, Nitrogen, and Phosphorus.
624 *Annu. Rev. Earth Planet. Sci.* **2018**, *46* (1), 521–548. [https://doi.org/10.1146/annurev-](https://doi.org/10.1146/annurev-earth-082517-010018)
625 [earth-082517-010018](https://doi.org/10.1146/annurev-earth-082517-010018).
- 626 (54) Douglas, P. M. J.; Pagani, M.; Eglinton, T. I.; Brenner, M.; Hodell, D. A.; Curtis, J. H.;
627 Ma, K. F.; Breckenridge, A. Pre-Aged Plant Waxes in Tropical Lake Sediments and
628 Their Influence on the Chronology of Molecular Paleoclimate Proxy Records. *Geochim.*
629 *Cosmochim. Acta* **2014**, *141*, 346–364. <https://doi.org/10.1016/j.gca.2014.06.030>.
- 630 (55) French, K. L.; Hein, C. J.; Haghypour, N.; Wacker, L.; Kudrass, H. R.; Eglinton, T. I.;
631 Galy, V. Millennial Soil Retention of Terrestrial Organic Matter Deposited in the Bengal
632 Fan. *Sci. Rep.* **2018**, *8* (1), 1–8. <https://doi.org/10.1038/s41598-018-30091-8>.
- 633 (56) Vonk, J. E.; Drenzek, N. J.; Hughen, K. A.; Stanley, R. H. R.; McIntyre, C.; Montluçon,
634 D. B.; Giosan, L.; Southon, J. R.; Santos, G. M.; Druffel, E. R. M.; Andersson, A. A.;
635 Sköld, M.; Eglinton, T. I. Temporal Deconvolution of Vascular Plant-Derived Fatty
636 Acids Exported from Terrestrial Watersheds. *Geochim. Cosmochim. Acta* **2019**, *244*,

- 637 502–521. <https://doi.org/10.1016/j.gca.2018.09.034>.
- 638 (57) Coppola, A. I.; Wiedemeier, D. B.; Galy, V.; Haghypour, N.; Hanke, U. M.; Nascimento,
639 G. S.; Usman, M.; Blattmann, T. M.; Reisser, M.; Freymond, C. V.; Zhao, M.; Voss, B.;
640 Wacker, L.; Schefuß, E.; Peucker-Ehrenbrink, B.; Abiven, S.; Schmidt, M. W. I.;
641 Eglinton, T. I. Global-Scale Evidence for the Refractory Nature of Riverine Black
642 Carbon. *Nat. Geosci.* **2018**, *11* (8), 584–588. <https://doi.org/10.1038/s41561-018-0159-8>.
- 643 (58) Burdige, D. J. Burial of Terrestrial Organic Matter in Marine Sediments: A Re-
644 Assessment. *Global Biogeochem. Cycles* **2005**, *19* (4), 1–7.
645 <https://doi.org/10.1029/2004gb002368>.
- 646 (59) Oros, D. R.; Simoneit, B. R. T. *Identification and Emission Factors of Molecular*
647 *Tracers in Organic Aerosols from Biomass Burning Part 1 . Temperate Climate*
648 *Conifers*; 2001; Vol. 16. [https://doi.org/10.1016/S0883-2927\(01\)00021-X](https://doi.org/10.1016/S0883-2927(01)00021-X).
- 649 (60) Venkatesan, M. I.; Kaplan, I. R. The Lipid Geochemistry of Antarctic Marine Sediments:
650 Bransfield Strait. *Mar. Chem.* **1987**, *21* (2844), 347–375. [https://doi.org/10.1016/0304-](https://doi.org/10.1016/0304-4203(87)90056-9)
651 [4203\(87\)90056-9](https://doi.org/10.1016/0304-4203(87)90056-9).
- 652 (61) Jiang, C.; Alexander, R.; Kagi, R. I.; Murray, A. P. Origin of Perylene in Ancient
653 Sediments and Its Geological Significance. *Org. Geochem.* **2000**, *31* (12), 1545–1559.
654 [https://doi.org/10.1016/S0146-6380\(00\)00074-7](https://doi.org/10.1016/S0146-6380(00)00074-7).
- 655 (62) Sánchez-Ramírez, S.; Wilson, A. W.; Ryberg, M. Overview of Phylogenetic Approaches
656 to Mycorrhizal Biogeography, Diversity and Evolution. In *Biogeography of Mycorrhizal*
657 *Symbiosis*; Tedersoo, L., Ed.; Springer International Publishing, 2017; Vol. 230, pp 1–
658 38. <https://doi.org/10.1007/978-3-319-56363-3>.
- 659 (63) Blumer, M. Organic Pigments : Their Long-Term Fate. *Science.* **1965**, *149* (3685), 722–
660 726. <https://doi.org/10.1126/science.149.3685.722>.

- 661 (64) Fernandez, C. W.; Langley, J. A.; Chapman, S.; McCormack, M. L.; Koide, R. T. The
662 Decomposition of Ectomycorrhizal Fungal Necromass. *Soil Biol. Biochem.* **2016**, *93*, 38–
663 49. <https://doi.org/10.1016/j.soilbio.2015.10.017>.
- 664 (65) Bianchi, T. S.; Cui, X.; Blair, N. E.; Burdige, D. J.; Eglinton, T. I.; Galy, V. Centers of
665 Organic Carbon Burial and Oxidation at the Land-Ocean Interface. *Org. Geochem.* **2018**,
666 *115*, 138–155. <https://doi.org/10.1016/j.orggeochem.2017.09.008>.
- 667 (66) Hedges, J. I.; Oades, J. M. Comparative Organic Geochemistries of Soils and Marine
668 Sediments. *Org. Geochem.* **1997**, *27* (7–8), 319–361. [https://doi.org/10.1016/s0146-](https://doi.org/10.1016/s0146-6380(97)00056-9)
669 [6380\(97\)00056-9](https://doi.org/10.1016/s0146-6380(97)00056-9).
- 670